POLITECNICO DI TORINO
Repository ISTITUZIONALE

A mesh-free adaptive parametric macromodeling strategy with guaranteed stability

Original
A mesh-free adaptive parametric macromodeling strategy with guaranteed stability / Zanco, A., Grivet-Talocia, S.. - ELETTRONICO. - (2020), pp. 1-6. (2020 International Symposium on Electromagnetic Compatibility - EMC EUROPE, EMC EUROPE 2020 Rome, Italy 2020) [10.1109/EMCEUROPE48519.2020.9245635].

Availability:
This version is available at: 11583/2920812 since: 2021-09-03T09:42:03Z

Publisher:
Institute of Electrical and Electronics Engineers Inc.

Published
DOI:10.1109/EMCEUROPE48519.2020.9245635

Terms of use:

This article is made available under terms and conditions as specified in the corresponding bibliographic description in the repository

Publisher copyright
IEEE postprint/Author's Accepted Manuscript

©2020 IEEE. Personal use of this material is permitted. Permission from IEEE must be obtained for all other uses, in any current or future media, including reprinting/republishing this material for advertising or promotional purposes, creating new collecting works, for resale or lists, or reuse of any copyrighted component of this work in other works.

(Article begins on next page)

14 October 2026

A mesh-free adaptive parametric macromodeling strategy with guaranteed stability

Alessandro Zanco, *Student Member, IEEE*, Stefano Grivet-Talocia, *Fellow, IEEE*

***Abstract*—This paper proposes a fully automated procedure for the generation of behavioral time-domain macromodels of complex multiport electric, electronic or electromagnetic systems, whose response depends on several design parameters. The latter are embedded in closed form in the macromodel structure through a mesh-free radial basis function representation, which allows scalability to a possibly large number of parameters. A greedy process is proposed to iteratively select a reduced number of training frequency responses, so that the macromodel accuracy is enforced uniformly in the parameter space. Examples with up to ten independent parameters demonstrate the effectiveness of proposed algorithm.**

I. Introduction

Behavioral macromodels are extensively used in numerical modeling and simulation for Signal-Power Integrity and Electromagnetic Compatibility. Due to availability of reliable and efficient rational curve fitting algorithms [1], generation of reduced-order behavioral models has become a routine task for designers, who are able to represent with compact time-domain equivalents the dynamic behavior of possibly complex electromagnetic multiport systems known through samples of their frequency responses.

This paper builds on recent developments on multivariate macromodeling [2]–[4], and proposes a practical and fully automated algorithm that generates parameterized behavioral models embedding in a closed form a dependence on several design parameters. The latter can be related to geometry, materials, parasitic elements, or even ambient quantities such as temperature. Availability of parameterized macromodels is a key enabling factor for running system-level optimization, design centering, what-if and sensitivity analysis since early stages of product development, while taking into account the full dynamic behavior of the structure under investigation, including parasitics.

Various methods have been presented for parameterized modeling [2]–[13]. Most of these approaches are however limited to a reduced number of independent parameters, due to the inherent structure of the model. For instance, all approaches that embed parameters through expansion into a set of basis functions for each individual parameter [3], [4] inevitably lead to a curse of dimensionality when multiple parameters are to be embedded. Such methods have been demonstrated to have an excellent performance in case of 2-3 parameters, for which both model generation through multivariate fitting and stability/passivity enforcement are feasible in a relatively reduced runtime. A larger number of parameters is impractical in this framework.

An attempt to remove the above limitation was performed in [14], [15], where mesh-free parameter representations were introduced through an expansion of model coefficients into Radial Basis Functions (RBF). The preliminary results in [14] demonstrated feasibility of this approach to improve scalability to a larger parameter space dimension, while preserving or enforcing uniform stability. However, no explicit guideline was provided to place the centers of the RBFs for optimal performance and/or accuracy. This paper solves this problem and provides a fully automated greedy process that, starting from a well-defined distribution of few RBF centers placed through a space-filling Sobol sequence [16], iteratively increases their number until model accuracy is under control throughout the parameter space. Compared to the adaptive sampling scheme based on passivity metrics presented in [17], the proposed approach removes the limitation of structured parameter bases, thus improving scalability.

The proposed algorithm is as simple as effective. In addition, enforcing positiveness of a reduced set of model coefficients, as in [3], [15], provably constrains all parameter-dependent macromodel poles to be stable throughout the parameter space, thus enabling time-domain usage of the models. Algorithm performance is here demonstrated on a significant number of test cases characterized by up to ten independent parameters.

II. Background and Notation

We summarize here some background concepts and the general macromodeling framework from which proposed algorithm is derived. We consider a P-port electrical, electronic or electromagnetic structure, represented by a linear or linearized (small-signal) system, whose response depends on a set of ρ independent parameters collected in vector $\boldsymbol{\vartheta} = [\vartheta^1, \ldots, \vartheta^\rho] \in \Theta$. Without loss of generality we assume Θ to be a unitary (normalized) ρ dimensional hyper-cube.

We assume that the structure is initially characterized through M parametric frequency responses, obtained through physics-based simulations (i.e. SPICE through a small-signal AC sweep in case of electronic circuits, or a frequency-domain field solver in case of an electromagnetic system). The m-th response includes K frequency samples $s_k = \mathrm{j}\omega_k$ and is denoted as $\breve{\mathbf{H}}(s_k, \boldsymbol{\vartheta}_m) = \breve{H}_{k,m}$, $k = 1, \ldots, K$, $m = 1, \ldots, M$. The construction of a parameterized reduced-order macromodel $\mathbf{H}(s, \boldsymbol{\vartheta})$ is achieved by enforcing the following fitting condition

$$\left\| \mathbf{H}(s_k, \boldsymbol{\vartheta}_m) - \breve{\mathbf{H}}_{k,m} \right\| \approx 0, \quad \forall k,\ m. \tag{1}$$

The adopted model structure is standard [18], [19]

$$\mathbf{H}(s; \boldsymbol{\vartheta}) = \frac{\mathbf{N}(s; \boldsymbol{\vartheta})}{D(s; \boldsymbol{\vartheta})} = \frac{\sum_{n=0}^{\bar{n}} \sum_{\ell=1}^{\bar{\ell}} \mathbf{R}_{n,\ell}\, \xi_\ell(\boldsymbol{\vartheta})\, \varphi_n(s)}{\sum_{n=0}^{\bar{n}} \sum_{\ell=1}^{\bar{\ell}} r_{n,\ell}\, \xi_\ell(\boldsymbol{\vartheta})\, \varphi_n(s)}. \tag{2}$$

where the free model coefficients, to be determined by solving (1), are $\mathbf{R}_{n,\ell} \in \mathbb{R}^{P\times P}$ and $r_{n,\ell} \in \mathbb{R}$. Each basis function $\varphi_n(s) = 1/(s-q_n)$ corresponds to the single partial fraction associated with a "basis" pole q_n, except $\varphi_0(s) = 1$. The basis poles are obtained through standard vector fitting [20] in a preprocessing phase. The terms $\xi_\ell(\boldsymbol{\vartheta})$ are multivariate basis functions that catch and embed the parameter variability in the model. As pointed out in [14], [15], mesh-free approaches based on RBF expansions seem to be very promising for high-dimensional parameterized macromodeling. Therefore, we will adopt Gaussian RBFs as basis functions

$$\xi_\ell(\boldsymbol{\vartheta}) = e^{-\varepsilon\left\|\boldsymbol{\vartheta}-\hat{\boldsymbol{\vartheta}}_\ell\right\|^2} \tag{3}$$

to represent parameter-induced variations, where the *shape parameter* ε determines the geometry of the RBF. Each $\xi_\ell(\boldsymbol{\vartheta})$ is basically a bell-shaped hyper-surface centered at $\hat{\boldsymbol{\vartheta}}_\ell$, having a width inversely proportional to $\sqrt{\varepsilon}$. In the proposed framework, the shape parameter ε is common to all the basis functions (for details see Section III) and the RBF centers $\hat{\boldsymbol{\vartheta}}_\ell$ are common to both numerator and denominator in (2).

The optimization problem in (1) is non-convex in the decision variables $\mathbf{R}_{n,\ell},\ r_{n,\ell}$. A standard relaxation strategy to solve (1) is the so-called *Parameterized Sanathanan-Koerner (PSK)* iteration [18], [19], [21]

$$\min \left\| \frac{\mathbf{N}^\mu(\mathrm{j}\omega_k;\boldsymbol{\vartheta}_m) - D^\mu(\mathrm{j}\omega_k;\boldsymbol{\vartheta}_m)\breve{\mathbf{H}}_{k,m}}{D^{\mu-1}(\mathrm{j}\omega_k;\boldsymbol{\vartheta}_m)} \right\|_F^2 \tag{4}$$

where $\mu = 1, 2, \ldots$ is the iteration index and F denotes the Frobenius norm. We recognize in (4) a linear re-weighted least square problem that can be solved with basic pseudo-inverse techniques. The iterations stop when the unknown coefficients $\mathbf{R}_{n,\ell}$ and $r_{n,\ell}$ stabilize.

The Gaussian RBFs (3) are positive definite, i.e., $\xi_\ell(\boldsymbol{\vartheta}) > 0$, $\forall \ell$ and $\forall \boldsymbol{\vartheta} \in \Theta$. As shown in [3], [14], [15], adopting such basis functions greatly simplifies the process of stability enforcement, since uniform macromodel stability can be guaranteed by subjecting denominator coefficients to simple linear inequality constraints, which are easily embedded within the PSK iteration (4).

The selection of the RBFs free parameters (shape factor and center) as well as the number of RBFs must be carefully tuned in order to accurately capture the parametric variability. The choice of an optimal shape parameter is still an open problem [22]. In this work, the optimal ε will be determined by a brute-force search while minimizing model data fitting error. The selection of RBF number and location of RBF centers is instead the main focus of this paper. Section III discusses a quasi-optimal strategy for their automated determination.

III. Greedy RBF center selection

The proposed greedy algorithm works iteratively. At each iteration $\nu = 0, 1, \ldots$, we denote the currently available model as $\mathbf{H}^\nu(s,\boldsymbol{\vartheta})$, with the corresponding model-data error at the m-th parameter location $\boldsymbol{\vartheta}_m$ as the worst-case RMS deviation among all transfer matrix elements

$$\mathcal{E}^\nu(\boldsymbol{\vartheta}_m) = \max_{i,j} \sqrt{\frac{1}{K}\sum_{k=1}^{K} \left| \mathbf{H}^\nu_{i,j}(\mathrm{j}\omega_k,\boldsymbol{\vartheta}_m) - (\breve{\mathbf{H}}_{k,m})_{i,j} \right|^2}. \tag{5}$$

As a general rule valid for all iterations, the set $\mathcal{M} = \{\boldsymbol{\vartheta}_1, \ldots, \boldsymbol{\vartheta}_M\}$ of all parameter values for which the frequency response is available as raw data is split into two mutually disjoint subsets $\mathcal{M}^t_\nu$ and $\mathcal{M}^v_\nu$ with m^t_ν and m^v_ν responses, respectively. We have $\mathcal{M} = \mathcal{M}^t_\nu \cup \mathcal{M}^v_\nu$ and $m^t_\nu + m^v_\nu = M$. The responses in set $\mathcal{M}^t_\nu$ are used as *training* data to construct and solve the PSK fitting system (4), whereas the responses in set $\mathcal{M}^v_\nu$ are used for model self-validation. A third set $\mathcal{M}^c_\nu \subset \mathcal{M}^t_\nu$ collects the m^c_ν RBF centers that contribute to the model structure. Therefore, each Gaussian RBF is centered at some parameter value for which the frequency response is available. To ensure a proper regression such that (4) is sufficiently overdetermined and thus prevent overfitting phenomena, we enforce that $m^t_\nu \geq 2\ m^c_\nu$ at all iterations. Once the RBF centers are fixed (see below), the RBF shape parameter ε is obtained at each iteration by a one-dimensional search that minimizes the worst-case model-data error (5) among all validation samples $\boldsymbol{\vartheta}_m \in\ \mathcal{M}^v_\nu$.

A. Initialization

In this work, we assume that the full set $\mathcal{M}$ is fixed a priori and is not augmented through iterations. It is thus necessary to choose the raw samples $\boldsymbol{\vartheta}_m$ so that they cover as uniformly as possible the high-dimensional parameter space. In this work, we generate these samples using a basic Latin Hypercube Sampling sequence [23], although other choices are possible (see examples in Section IV).

In the initialization phase $\nu = 0$, it is necessary to split $\mathcal{M}$ into training and validation samples. Also the training samples should span the entire parameter space, in order to control the model-data error as uniformly as possible. For this reason, we consider a truncated ρ-dimensional Sobol sequence [16] with m^t_0 points

$$\mathcal{S}^t = \{\mathbf{s}_i :\ \ i = 1, \ldots, m^t_0\}. \tag{6}$$

The initial training samples are selected as the m^t_0 elements of $\mathcal{M}$ that form the set of nearest neighbors to $\mathcal{S}^t$.

The same process is used to select the m^c_0 centers from the training samples $\mathcal{M}^t_0$. It turns out that, if the same random seed is used to generate the two Sobol sequences pertaining to training samples and RBF centers, it is sufficient to select as RBF centers the first m^c_0 elements of $\mathcal{M}^t_0$.

B. Adaptive refinement

Let us assume that iteration ν is completed, model $\mathbf{H}^\nu(s,\boldsymbol{\vartheta})$ is available as well as the sets collecting RBF centers $\mathcal{M}^c_\nu$, training samples $\mathcal{M}^t_\nu$, and validation samples $\mathcal{M}^v_\nu$. We first evaluate the error function $\mathcal{E}^\nu(\boldsymbol{\vartheta}_m)$ at all current validation samples in $\mathcal{M}^v_\nu$. A new candidate RBF center $\tilde{\boldsymbol{\vartheta}}^\nu$ is then selected through

$$\tilde{\boldsymbol{\vartheta}}^\nu = \arg \max_{\boldsymbol{\vartheta}_m \in \mathcal{M}^v_\nu} \mathcal{E}^\nu(\boldsymbol{\vartheta}_m) \tag{7}$$

as the particular validation sample where the model-data error is largest. Finally, the sets $\mathcal{M}_\nu^t$, $\mathcal{M}_\nu^v$, $\mathcal{M}_\nu^c$ are updated as

$$\begin{aligned}\mathcal{M}_{\nu+1}^t &= \mathcal{M}_\nu^t \cup \tilde{\boldsymbol{\vartheta}}^\nu \\ \mathcal{M}_{\nu+1}^c &= \mathcal{M}_\nu^c \cup \tilde{\boldsymbol{\vartheta}}^\nu \\ \mathcal{M}_{\nu+1}^v &= \mathcal{M}_\nu^v \setminus \tilde{\boldsymbol{\vartheta}}^\nu\end{aligned} \tag{8}$$

Once these sets are updated, the model is constructed by solving (4) while optimizing the Gaussian shape parameter ε.

The adaptive algorithm stops at a certain iteration $\bar{\nu}$ when, given an error threshold $\mathcal{E}_{\max}$, it holds that

$$\max_{\boldsymbol{\vartheta}_m \in \mathcal{M}_{\bar{\nu}-1}^v} \mathcal{E}^{\bar{\nu}}(\boldsymbol{\vartheta}_m) < \mathcal{E}_{\max} \tag{9}$$

Additionally, to prevent the algorithm from adding too many RBFs, we require that the number of added samples (iterations) never exceeds a prescribed maximum $\nu_{\max}$. The greedy RBF selection algorithm is summarized below in form of pseudo-code.

Algorithm 1 Adaptive RBFs center selection

Require: Parametric dataset $\mathcal{M}$
Require: Control parameters $\mathcal{E}_{\max}$, $\nu_{\max}$, m_0^t, m_0^c
1: Populate $\mathcal{M}_0^t$, $\mathcal{M}_0^c$ as described in Sec. III-A
2: Set $\mathcal{M}_0^v = \mathcal{M} \setminus \mathcal{M}_0^t$
3: Set $\nu = 0$
4: **repeat**
5: Generate model $\mathbf{H}^\nu(s, \boldsymbol{\vartheta})$ on training samples $\mathcal{M}_\nu^t$
6: Evaluate error function $\mathcal{E}^\nu(\boldsymbol{\vartheta}_m)$, $\forall \boldsymbol{\vartheta}_m \in \mathcal{M}_\nu^v$
7: Define new RBF center $\tilde{\boldsymbol{\vartheta}}^\nu$ as in (7)
8: Update sets $\mathcal{M}_\nu^t$, $\mathcal{M}_\nu^v$, $\mathcal{M}_\nu^c$ as in (8)
9: Update iteration index $\nu = \nu + 1$
10: **until** $\mathcal{E}^\nu(\boldsymbol{\vartheta}_m) < \mathcal{E}_{\max}$, $\forall \boldsymbol{\vartheta}_m \in \mathcal{M}_\nu^v$ or $\nu = \nu_{\max}$
11: **return** Final model $\mathbf{H}^{\bar{\nu}}(s, \boldsymbol{\vartheta})$

IV. Examples

The proposed algorithm is now tested on a significant set of test cases, characterized by a number of independent parameters ranging from $\rho = 2$ up to $\rho = 10$.

A. A linearized buffer model

The first example we consider is a linearized model of a buffer, parameterized by its bias voltage $V_{\text{dd}} \in [0.5,\ 1.5]$ V and the operation temperature $T = [20,\ 50]\ ^\circ C$. The initial dataset includes $M = 341$ parametric frequency responses obtained by small-signal AC sweeps in a circuit solver, arranged in a 11×31 Cartesian lattice. Each response includes $K = 274$ frequency samples in the band $f_{\min} = 0$ Hz, $f_{\max} = 10$ THz (to show high-frequency asymptotic behavior).

The adaptive algorithm is set-up with $m_0^t = 20$, $m_0^c = 10$, a maximum allowed number of RBFs to be added $\nu_{max} = 30$, and error threshold $\mathcal{E}_{\max} = 10^{-2}$. With these settings and a number of poles $\bar{n} = 5$, the presented method is able to extract an accurate and uniformly stable model, with a worst-case absolute error on validation samples is 9.31×10^{-3}, selecting only 6 additional RBFs. A comparison between model and data responses is provided in Fig 1.

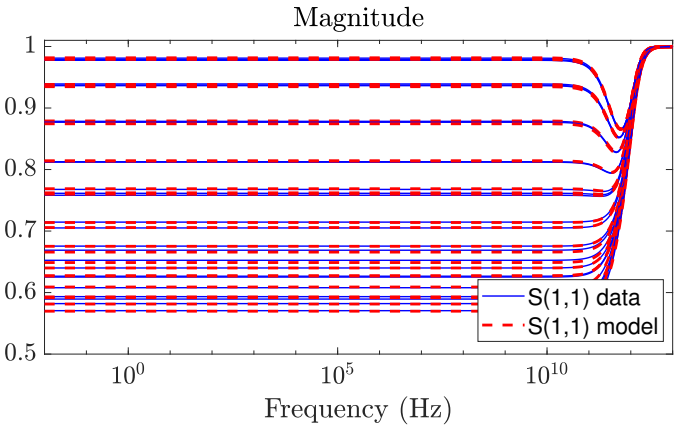

Fig. 1. Validation of the buffer model (red-dotted line) compared to raw data (blue solid line).

The panels in Fig. 2 depict the distribution of the error function on the parameter space for 4 adaptive refinement iterations. As expected, the adaptive algorithm places additional RBFs (red dots) in correspondence of large model-data error occurrences, until a uniformly accurate model is obtained.

The total CPU time required by the algorithm to adaptively select new RBFs centers is 6 minutes. Approximately, more than half of the computational time is required to choose the optimal value of the shape-parameter ε.

B. A Low-Noise Amplifier

In this second example we consider a Low-Noise Amplifier (see [24] for a schematic), whose constitutive parameters (originally reported in [15]) are listed in Table I. Parameters C_* and L_* are transistor parasitics, the remaining parameters are transmission line substrate and conductor thickness, and conductor width. The value of the i-th parameter is contained within a 20% band, centered on the nominal value $\bar{\vartheta}_i$

TABLE I
LNA parameters (see text)

#	Parameter ϑ_i	$\bar{\vartheta}_i$
1	L_b	1.1 nH
2	L_c	1.1 nH
3	L_e	0.25 nH
4	C_{cb}	0.0020 pF
5	C_{be}	0.08 pF
6	C_{ce}	0.08 pF
7	h	0.5 mm
8	t_k	2.0 μm
9	$w_{1,2,3}$	0.25 mm
10	w_4	0.8 mm

In order to assess scalability of our framework, we tested the presented algorithm on three different parameterizations (ϑ_i identifies that parameters as in Table I): $\rho = 5$ parameters (ϑ_1 to ϑ_5), $\rho = 8$ parameters (ϑ_1 to ϑ_8), and $\rho = 10$ parameters (ϑ_1 to ϑ_{10}). The training and validation datasets have been generated according to a Latin Hypercube Sampling scheme,

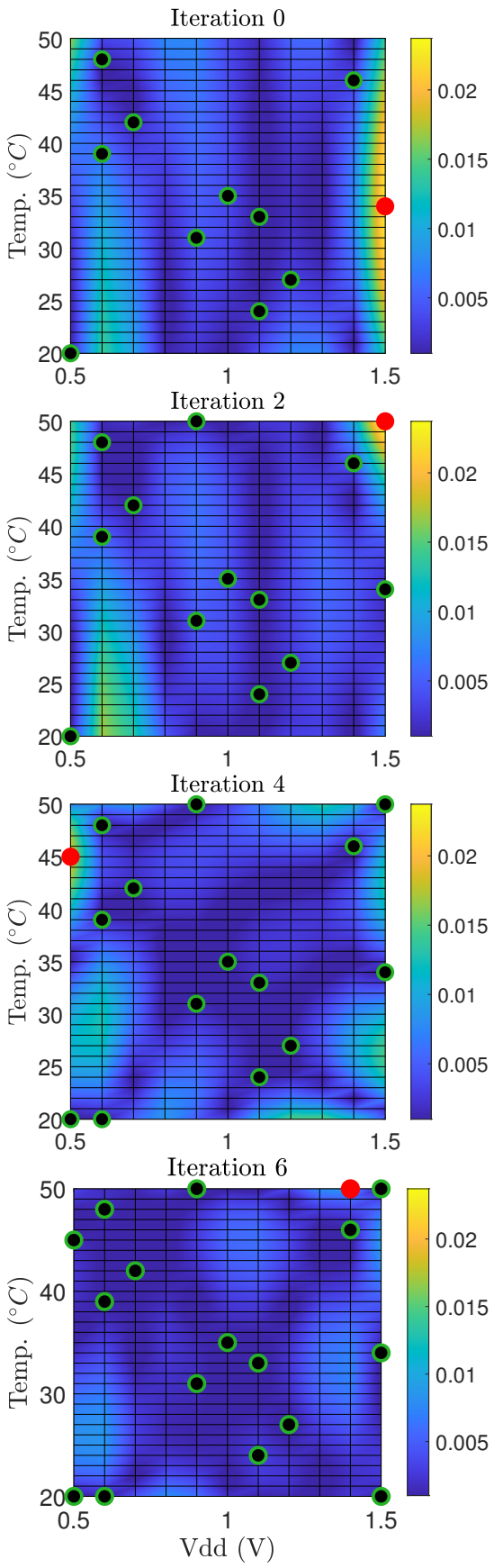

Fig. 2. Buffer model vs data error for some relevant algorithm iterations. Black dots depict the location of current RBF centers; red dots denote candidate new RBF centers.

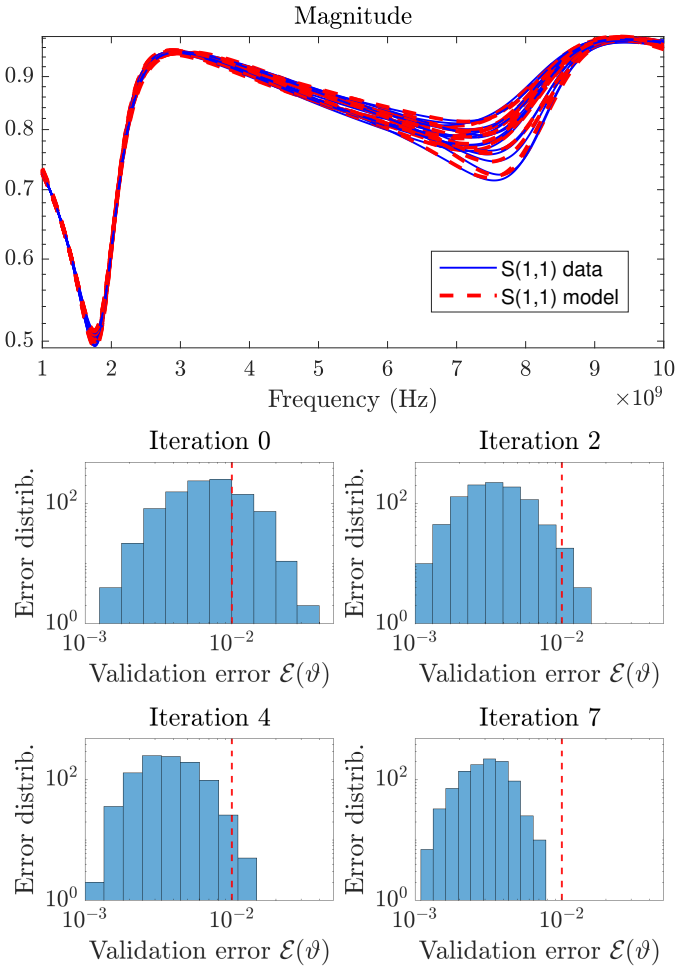

Fig. 3. LNA model with $\rho = 5$ parameters. Top panel: model-data comparison for a set of randomly selected validation data. Bottom panel: distribution of validation error at 4 adaptive iterations. The red-dotted lines represent the target error threshold $\mathcal{E}_{\max}$.

ensuring that the total number of samples $M = m_0^t + m_0^v = 200\rho$ scales only linearly with the parameter space dimension. Each dataset includes $K = 701$ frequency samples in the band [1 Hz, 10 GHz].

In high-dimensional spaces it is not possible to represent the error function as in Fig. 2. Thus, in the following examples we will visualize progress of the algorithm through iterations by means of histograms representing the error function distribution when evaluated on validation samples. For all the examples, the algorithm has been set with $\nu_{max} = 30$ and $\mathcal{E}_{\max} = 10^{-2}$.

1) $\rho = 5$ parameters: This structure is parameterized only by lumped parameters, making the induced variability fairly sample to catch. We expect the initial number of required RBF centers m_0^c to be small, thus we set $m_0^c = 7$ and $m_0^t = 14$. The number of model poles is $\bar{n} = 14$.

The presented greedy algorithm added 7 adaptively centered RBFs (for an overall CPU time of 7 minutes) to obtain a uniformly stable model, whose worst-case absolute error evaluated on the remaining $m_0^v = 979$ validation samples is 7.71×10^{-3}. Model responses compared to data are reported in the top panel of Fig. 3. The histograms in the bottom

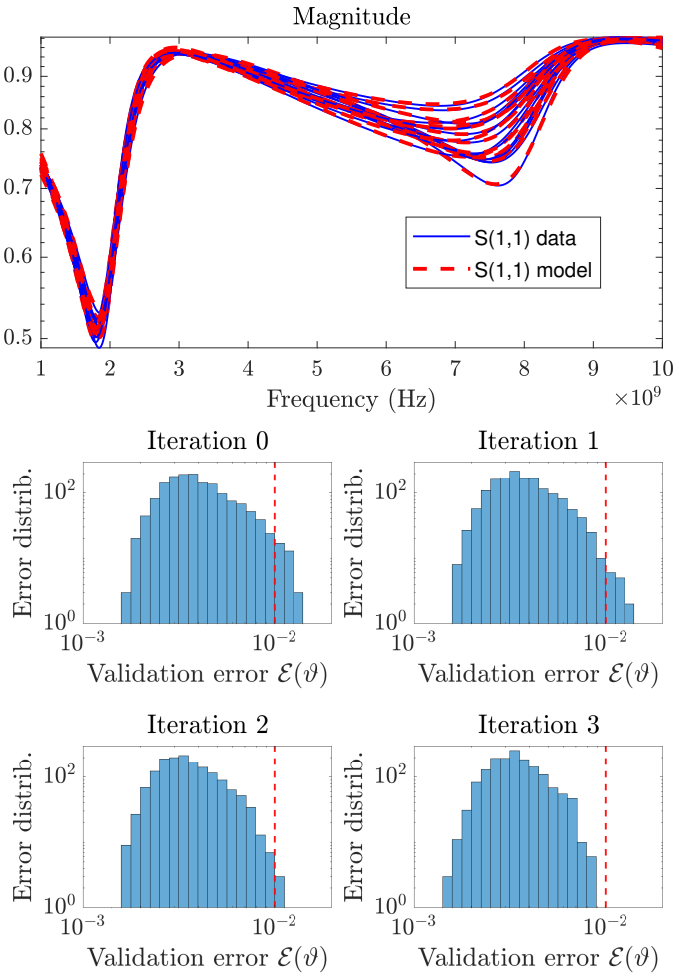

Fig. 4. As in Fig. 3, but for the LNA case with $\rho = 8$ parameters.

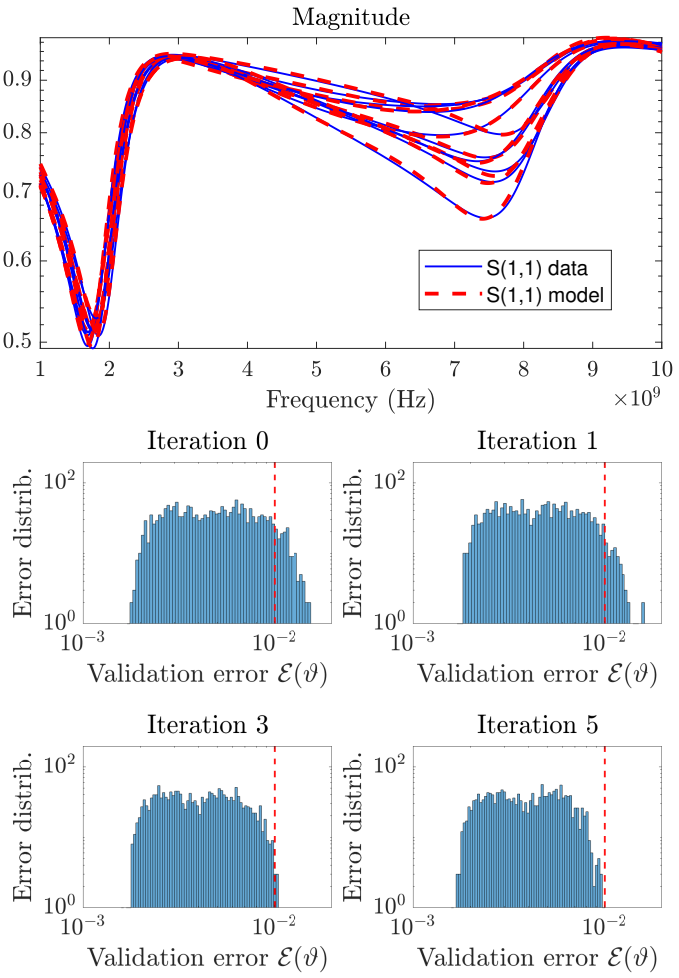

Fig. 5. As in Fig. 3, but for the LNA case with $\rho = 10$ parameters.

panel depict the distribution of the error throughout validation samples for four different iterations. We see that, as additional RBFs are adaptively positioned, the error distribution moves to the left, until it is uniformly below the given error threshold. Assuming to know a-priori the optimal shape parameter value and skipping the corresponding optimization step, the required CPU time reduces to only 2 minutes.

2) $\rho = 8$ parameters: Differently from previous example, this scenario includes two distributed parameters, namely the substrate and conductor thickness of feeding transmission lines, requiring a larger number of initial RBFs to better track the induced variability. We start with $m_0^c = 35$ and $m_0^t = 70$. With a number of poles $\bar{n} = 16$, the adaptive algorithm took only 3 iterations to extract an accurate and uniformly stable model, for a CPU time of 14 minutes. In case the optimal shape parameter is known and no iterative search is performed, the computational cost is reduced to 5 minutes.

The model worst-case absolute error evaluated at the remaining 1527 validation samples is 8.93×10^{-3}. Figure 4 compares the model responses to data for a randomly chosen set of validation samples and provides the error distribution throughout validation samples.

3) $\rho = 10$ parameters: In this last example, we account for all LNA parameters in Table I, including transmission-line conductor widths w_*. The additional complexity introduced by these two latter parameters requires a larger initial number of RBFs, that we set to $m_0^c = 67$ with $m_0^t = 134$ training samples, with a number of model poles $\bar{n} = 16$. The proposed algorithm required 41 minutes to place 5 additional RBFs and obtain a final uniformly stable model, whose worst-case absolute error on the remaining 1862 validation samples is 9.90×10^{-3}.

Figure 5 compares the model responses with raw data for a randomly selected subset of validation samples and depicts the evolution of the error distribution through iterations. Also in this case, the overall computational time reduces to approximately 30 minutes if the search on the shape parameter ε is skipped.

These results show that, even in high-dimensional parameter spaces, the adopted mesh-free representation based on RBFs allows to reach the target accuracy $\mathcal{E}_{\max}$ with the addition of few automatically positioned RBFs. Furthermore, in all the reported examples we observed that most of the computational effort is devoted to choosing a suitable value for the RBF shape parameter ε. Thus, developing a suitable heuristic to estimate ε without the need of any iterative search would greatly improve the performance of the presented algorithm. This is the subject of our current investigations.

V. Conclusions

This paper introduced a greedy process for the automated generation of parameterized macromodels. The main novel contribution is a simple yet effective iterative process for the determination of few radial basis functions and associated training samples from which a sparse model representation is computed. Thanks to suitable inequality constraints embedded in the model identification process, all parameterized model poles are guaranteed to be stable. The mesh-free nature of the model parameterization allows for scalability to several independent parameters. Excellent results in terms of accuracy and reduced model complexity are here demonstrated for up to ten parameters.

References

[1] S. Grivet-Talocia and B. Gustavsen, *Passive macromodeling: Theory and applications*. John Wiley & Sons, 2015, vol. 239.

[2] S. Grivet-Talocia, "A perturbation scheme for passivity verification and enforcement of parameterized macromodels," *IEEE Transactions on Components, Packaging and Manufacturing Technology*, vol. 7, no. 11, pp. 1869–1881, 2017.

[3] S. Grivet-Talocia and R. Trinchero, "Behavioral, parameterized, and broadband modeling of wired interconnects with internal discontinuities," *IEEE Transactions on Electromagnetic Compatibility*, vol. 60, no. 1, pp. 77–85, 2018.

[4] A. Zanco, S. Grivet-Talocia, T. Bradde, and M. De Stefano, "Enforcing passivity of parameterized lti macromodels via hamiltonian-driven multivariate adaptive sampling," *IEEE Transactions on Computer-Aided Design of Integrated Circuits and Systems*, vol. 39, no. 1, pp. 225–238, 2018.

[5] F. Ferranti, L. Knockaert, and T. Dhaene, "Parameterized s-parameter based macromodeling with guaranteed passivity," *IEEE Microwave and Wireless Components Letters*, vol. 19, no. 10, pp. 608–610, 2009.

[6] F. Ferranti, T. Dhaene, and L. Knockaert, "Compact and passive parametric macromodeling using reference macromodels and positive interpolation operators," *Components, Packaging and Manufacturing Technology, IEEE Transactions on*, vol. 2, no. 12, pp. 2080–2088, Dec 2012.

[7] F. Ferranti, L. Knockaert, and T. Dhaene, "Guaranteed passive parameterized admittance-based macromodeling," *Advanced Packaging, IEEE Transactions on*, vol. 33, no. 3, pp. 623–629, Aug 2010.

[8] ——, "Parameterized S-parameter based macromodeling with guaranteed passivity," *Microwave and Wireless Components Letters, IEEE*, vol. 19, no. 10, pp. 608–610, Oct 2009.

[9] ——, "Passivity-preserving parametric macromodeling by means of scaled and shifted state-space systems," *IEEE Transactions on Microwave Theory and Techniques*, vol. 59, no. 10, pp. 2394–2403, 2011.

[10] S. Grivet-Talocia and E. Fevola, "Compact parameterized black-box modeling via fourier-rational approximations," *IEEE Transactions on Electromagnetic Compatibility*, vol. 59, no. 4, pp. 1133–1142, 2017.

[11] E. R. Samuel, L. Knockaert, F. Ferranti, and T. Dhaene, "Guaranteed passive parameterized macromodeling by using sylvester state-space realizations," *IEEE Transactions on Microwave Theory and Techniques*, vol. 61, no. 4, pp. 1444–1454, 2013.

[12] A. Antoulas, A. Ionita, and S. Lefteriu, "On two-variable rational interpolation," *Linear Algebra and its Applications*, vol. 436, no. 8, pp. 2889 – 2915, 2012.

[13] Y. Q. Xiao, S. Grivet-Talocia, P. Manfredi, and R. Khazaka, "A novel framework for parametric loewner matrix interpolation," *IEEE Transactions on Components, Packaging and Manufacturing Technology*, vol. 9, no. 12, pp. 2404–2417, 2019.

[14] A. Zanco and S. Grivet-Talocia, "High-dimensional parameterized macromodeling with guaranteed stability," in *2019 IEEE 28th Conference on Electrical Performance of Electronic Packaging and Systems (EPEPS), Montreal (Canada), 6–9 Oct.*, 2019, pp. 1–4 (in press).

[15] A. Zanco, S. Grivet-Talocia, T. Bradde, and M. De Stefano, "Uniformly stable parameterized macromodeling through positive definite basis funtions," *IEEE Transactions on Components, Packaging and Manufacturing Technology*, 2020, submitted.

[16] P. Bratley and B. L. Fox, "Algorithm 659: Implementing Sobol's quasirandom sequence generator," *ACM Transactions on Mathematical Software (TOMS)*, vol. 14, no. 1, pp. 88–100, 1988.

[17] E. Fevola, A. Zanco, S. Grivet-Talocia, T. Bradde, and M. De Stefano, "An adaptive sampling process for automated multivariate macromodeling based on hamiltonian-based passivity metrics," *IEEE Transactions on Components, Packaging and Manufacturing Technology*, vol. 9, no. 9, pp. 1698–1711, Sep. 2019.

[18] D. Deschrijver, T. Dhaene, and D. De Zutter, "Robust parametric macromodeling using multivariate orthonormal vector fitting," *IEEE Transactions on Microwave Theory and Techniques*, vol. 56, no. 7, pp. 1661–1667, July 2008.

[19] P. Triverio, S. Grivet-Talocia, and M. S. Nakhla, "A parameterized macromodeling strategy with uniform stability test," *IEEE Trans. Advanced Packaging*, vol. 32, no. 1, pp. 205–215, Feb 2009.

[20] B. Gustavsen and A. Semlyen, "Rational approximation of frequency domain responses by vector fitting," *Power Delivery, IEEE Transactions on*, vol. 14, no. 3, pp. 1052–1061, jul 1999.

[21] C. Sanathanan and J. Koerner, "Transfer function synthesis as a ratio of two complex polynomials," *Automatic Control, IEEE Transactions on*, vol. 8, no. 1, pp. 56–58, jan 1963.

[22] M. Mongillo, "Choosing basis functions and shape parameters for radial basis function methods," *SIAM undergraduate research online*, vol. 4, pp. 190–209, 2011.

[23] M. D. McKay, R. J. Beckman, and W. J. Conover, "Comparison of three methods for selecting values of input variables in the analysis of output from a computer code," *Technometrics*, vol. 21, no. 2, pp. 239–245, 1979.

[24] T. Buss, "2 GHz low noise amplifier with the BFG425W," Philips Semiconductors, B.V., Nijmegen, The Netherlands, Tech. Rep., 1996. [Online]. Available: http://application-notes.digchip.com/004/4-7999.pdf